Eroding coastal sandy barriers under changing aeolian flux in the Gulf of Tunis

Oula Amrouni, Hodan Ibrahim Said, Abderraouf Hzami, Hechmi Missaoui, Gil Mahe, Essam Heggy

INSTM Bulletin
Marine and Freshwater Sciences

Vol. 48, 2023, 37-48

Research Article

Eroding coastal sandy barriers under changing aeolian flux in the Gulf of Tunis

Oula AMROUNI *[1], Hodan IBRAHIM SAID [1], Abderraouf HZAMI [1], Hechmi MISSAOUI, Gil MAHE [1, 2] & Essam HEGGY [3, 4]

[1] University of Carthage. National Institute of Marine Sciences and Technologies, Laboratory of Marine Environment
[2] University of Montpellier. HydroSciences Montpellier. Laboratory, IRD, CNRS
[3] University of Southern California. Viterbi School of Engineering. Los Angeles, CA, USA
[4] California Institute of Technology. Jet Propulsion Laboratory. Pasadena, CA, USA

***Correspondence:** oula.amrouni@instm.rnrt.tn

Received: 15/12/2022; **Accepted**: 11/07/2023; **Published**: 28/08/2023

Abstract: Sandy barriers are coastal features formed and reworked by terrestrial and marine-induced processes along decadal to millenary scale periods**.** In the semi-arid areas along the extended North African coast, these coastal landscapes are undergoing accelerated morphodynamical changes induced by intensifying anthropogenic and climate drivers in the last century. To quantify the latter, we assess the changes in sediment dynamics of the Ghar El Melh sandy barrier extended over the northern part of the Gulf of Tunis in Tunisia using sedimentological analysis and quantification of the aeolian flux. A total of 37 subsurface samples and 30 surface aeolian trapped ones were collected at the coastal dunes of Ghar El Melh. Our sedimentological analysis reveals a distribution of 97% of sandy sediments and 3% of silty facies. The modal statistical analysis suggests that there are three distinguishable sediment types with 87% of samples formed by fine sands with modal value of 0.16 mm. The mixture of these indicates mixed terrigenous and marine sources redistributed by the hydrodynamic processes. The measurement of the aeolian flow suggests a maximum value of 0.0022 $kg.m.^{-1}min^{-1}$ which occurs in dust storms. This study reveals the low detrital sand supplies to the lagoon-sea barrier of Ghar El Melh, results in its gradual submersion, further exposing the coastal lagoon and engendering severe ecological degradations.

Keywords: Sand banks; Sedimentation; Coastal erosion; Eolian dust; submerged shorelines; Mediterranean Sea.

1. Introduction

Sandy barriers are shore-parallel accumulations of detrital sediments driven by fluvial, marine, or aeolian processes (Shepherd & Hesp, 2003; Edward J. Anthony, 2008). They are connected to the mainland enclosing wetland systems such as lagoons, saltmarshes, and sabkhas. The origin of sandy ridges can be

associated with the immersion of marine sandbars or the progradation of an estuarine/deltaic inlet by the longshore drift. Due to their low elevation, those coastal landforms are frequently submerged by sea waves and tidal processes and are heavily impacted by storm surges. The AR6 IPCC report (IPCC, 2022) suggested that the low-lying coastal areas are particularly threatened by the global sea level rise (SLR), especially in the semi-arid North African coastline along the southern part of the Mediterranean basin. Therefore, the forecasted impacts of the rising sea levels on North African sandy beaches increase the vulnerability of coastal areas to natural disasters (Lazzari et al., 2021; Corbau et al., 2022; Komi et al., 2022). Global climatic changes are also suggested to increase dust storm frequencies and intensities (Krasnov et al., 2016) in arid and semi-arid areas. The cumulative effect of these natural hazards is accentuated in low-lying urban coastal areas (Vousdoukas et al., 2020). As such, understanding the evolution of sandy coastal barriers in the vicinity of highly populated areas in northern Tunisia provides unique insights for long-term effective coastal management and, therefore, for improved resilience to coastal hazards for several communities. To achieve this objective, we study the sediment dynamic of the Ghar El Melh sandy barrier, particularly on quantifying the aeolian processes that govern the sand flux budget as detailed below.

2. Materials and Methods

2.1. Physical setting

Our study area is located on the northeastern coast of the western Gulf of Tunis in Tunisia in the central part of the Mediterranean basin (Figure 1 (A)). It is bordered to the north by the sea-lagoon connecting channel and to the south by the old course of the Medjerda River (Figure 1 (B,C)). Our study area is a sandy barrier formed by the sea wave and tides reworking of the terrestrial Mio-Plio-Quaternary inputs (Pimenta, 1959; Paskoff, 1994) of the Medjerda River during the ~1700 AC period (Delile et al., 2015). The sandy barrier, named herein after Ghar El Melh Sandy Barrier (GMSB), extends over 6 km of the coastline and within a foreshore width of 9 to 155 m. The main geomorphological features are an irregular vegetated dune, sand sheets, washover, tidal channel, and salt marsh.

The study area is under a semi-arid Mediterranean climate and characterized by seasonal wind direction. The average annual precipitation varies between 200 to 1000 mm y^{-1}, with a monthly rate of 2 to 90 mm during the summer and winter seasons, respectively (INM, 2020). The Ghar El Melh coast is characterized by a humid and fresh wind blowing from the north-westerly winds from Atlantic low-pressure polar fronts to East directions with an average speed of 11 $m.s^{-1}$ during the winter season, while during the summer period, the winds are dry blowing from the east-north-east sector with an average speed of 10 $m.s^{-1}$ (INM, 2019). The dominant longshore drift comes from the northeast to the southwest in winter and from the south to the north in summer (INM, 2019). The beach is under a microtidal regime (< 2 m) and falls within the dissipative morphodynamic classification (Hzami et al., 2021).

2.2. Sedimentary analysis

The sedimentological sampling campaign was carried out during the spring season (26 May 2021) over the littoral zone extending from the backshore to the foreshore areas of the GMSB, (Figure 1 (B)). A total of 37 subsurface sediment samples (CB 1 to CB 37) were collected along 11 profiles spaced by 500 m along the 5 km of coastline, on the dune field, the intertidal and the swash zones (Figure 1 (B,C)).

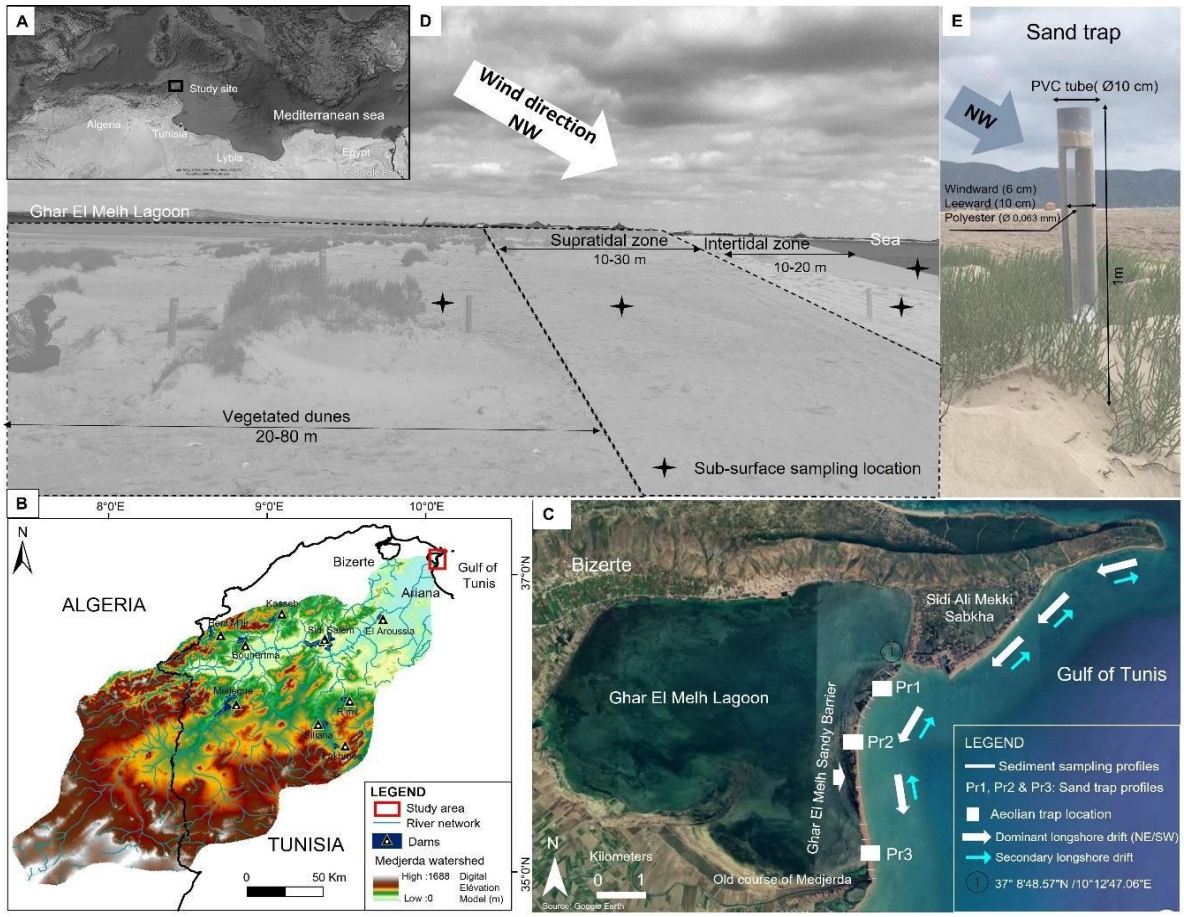

Figure 1. (A) Contextual location of the study site (B) The watershed of the Medjerda River; (C) The Ghar El Melh Sandy Barrier (GMSB) southeast of Bizerte; (D) Foreshore survey setup; (E) Example of aeolian sand traps deployed on the site.

2.2.1. Granulometry

Sediment samples underwent a granulometric analysis by sieving along the AFNOR sieve column. We calculate the grain-size indexes, e.g., the Modal value (Mo), the median grain size in Phi units (Φ) (MZ), the Standard deviation (σ), the Skewness (SKI), Kurtosis (Ku) from semi-logarithm curves, according to Folk and Ward (1957). The Sedimentary Types (ST) are statistically calculated to define the Source-to-Sink (Barusseau, 2011; Amrouni et al., 2019a). The particle size measurement of the muddy distribution within the range of 0.01-1000 µm was undertaken by The Malvern Mastersizer 2000.

2.2.2. Grain-shape description

Determining the source and the agent of sediment transport in a transitional environment is based on the beach samples' morphoscopic method (Cailleux, 1942). The grained-sand observation and surface texture identification were made under the 'LED Binocular Digital Microscope'. The observed features of the quartz are recognized as the most frequent and resistant beach component. The observed beach grain size ranged from 0.160 to 0.25 mm. The classification of the roundness types of the quartz grain, according to Krumbein (1941) is the fresh angular (NU), round mat (RM), sub-angular grain (SA), and moderately high-energy, blunted glow (BG) grain removed by water

in both fluviatile and/or marine environment.

2.2.3. Aeolian flux

The aeolian flux measurement occurred during the May 28, 2021, dust storm. The blowing winds came from the north-northwest to northeast directions with wind velocity exceeding 35 km.h^{-1} (9.7 m.s^{-1}). We used the saltation trap of "Leatherman type" (Krumbein, 1941) within a plastic tube of 1 m in length and diameter of 10 cm. The upper part of the tube is half open with two windows 6 cm wide facing the wind flux and a width of 10 cm towards the downwind lee face covered with a 63-um geotextile (Figure 1 (D)). The principle of the measurements is to collect the aeolian particle in the upper beach (HP), the dune feet (DF), the dune summit (SD), and along the sandy barrier, each 15 to 30 min. Sand traps are fixed along the cross-shore in the dune summit, the dune feet, and the upper beach. A total of 30 aeolian samples were collected by the sand traps and sieved.

The studied variables of the aeolian processes in the coastal environment are the wind directions, velocities, and frequencies, the median grain size of the trapped particles, and the coastal morphological characteristics. The measured flux rates Q_{mes} (kg.m^{-1}.mn^{-1}) of each run is compared to the semi-empirical model flux rate Q_{Cal} of Bagnold, 1941, Zingg, 1953, and Williams, 1964.

To calculate the optimal theoretical flux, the shear velocity u*, also expressed as the particle motion threshold speed, was determined at each height of the trap (z), based on Von Kármán formula (Von Kármán, 1921):

$$\ln z = k \times (Uz / u^*) + \ln z_0 \quad (1)$$

Where:

Uz = Wind speed average at altitude z (m.s^{-1}). u* = Shear velocity (m/s).

κ = Von Karman constant equal to 0.41.

z_0 = Roughness length (m) estimated at 1 mm (from Arens, 1997).

We calculated the Discrepancy Ratio (Dr) (Equation 2), of Sherman et al., (1993) to determine the most suitable aeolian sand transport formulas (Q_{cal}) for the study sector measurements (Q_{mes}) (Table 1) and measured aeolian flux in situ.

$$Dr = Q_{Cal}/Q_{mes} \quad (2)$$

Table 1: The semi-empirical flux models (Q_{Cal}) calculated by Bagnold (1936), Zingg (1953), and Williams (1964) and adopted for the study field in the Ghar El Melh beaches, Gulf of Tunis, Mediterranean.

Q_{Cal}= Calculated aeolian sediment flux; D50 = Grain size average (0.25 mm); d =Median grain size of the sediment (mm); ρa: Air density; u* = Shear velocity (m.s^{-1}); g = Gravity (m.s^{-2}).

	Formula	Variables
Bagnold, 1941	$QCal = B\frac{\rho a}{g}\sqrt{\frac{d}{D}}u*^3$	B= 0.118
Zingg, 1953	$QCal = K(\frac{D50}{d})^{0.75}\frac{\rho a}{g}u*^3$	K = 0.83
Williams, 1964	$QCal = a'\frac{\rho a}{g}u*^b$	a' = 1.189; b =3.422

3. Results

We subdivide our study area into three compartments from the north to the southern embayed coasts according to the geomorphology of the beaches along the GMSB:

- The northern area from the new channel to the historic channel (HC) (CB26 to CB37).
- The center area extends from the (HC) to the middle of the barrier (CB15 to CB25).
- The southern area stretches from the old mouth of Medjerda to the center of the GMSB (CB1 to CB14).

3.1. Sedimentological evolution

The results of the sedimentological analysis of the study area are listed in Table 2.

The textural analysis of the sediments of the GMSB shows that the sediments are characterized by sandy type (>0.063 mm)

in 97% of the cases. The muddy distribution (silt and clay) within a grain size less than 0.063 mm represents 3% of the samples (Table 1). All sandy sediment distributions are unimodal with a modal value Mo ranging between 0.160 mm (86%) and 0.250 mm (9%). The statistical modal calculation is shown in Figure 2.

We distinguished three Statistical Types:

- STI represents the main sediment distribution in 87% of the cases. It forms fine sand with a Mo value of 0.16 mm.
- STII was found in the coastal dune in 10% of cases, a medium sand type with a Mo value of 0.25 mm.
- STIII was found in the muddy sample collected from the submerged deltaic sediment, within 3% of the collected samples.

At the northern area of the sandy barrier, the grain size parameters reveal that the foreshore sediment is mainly composed of fine sand with Mz values ranging between 2,06 and 2,41 phi units (Φ). The medium sand with Mz values of 1,80 to 1,96 Φ is found in the samples CB27, CB31 et CB35 in the swash zone (Table 2). Sand distributions are very well sorted with an asymmetry to the fine tail for 42% of the cases, and 33% of samples are asymmetric for the coarser sizes and 25% symmetric.

At the center of the study area, the granulometric analysis suggests that sediments (CB15 to CB25) are characterized by a fine sand type with a median value Mz ranging between 2,00 to 2,36 Φ (0.20 < Md < 0.25 mm), which are very well to well sorted (0,27< σ < 0,36 Φ). The SKI parameter shows that 55% of the samples are asymmetric to the coarser fraction, 27% are asymmetric to the fine size, and 18 % present a symmetric distribution.

In the southern area, located in the old delta of the Medjerda River, sediments are mainly composed of fine-grained sand in 92% of the cases with a Mean Mz ranging from 2 to 2.38 Φ units, and medium-grained sand in 8% (Mean Mz size value of 1.97 Φ units). Sediment distributions are well to very well sorted, mostly symmetrical, and positively skewed.

Table 2. The grain size parameters result of the sandy barrier of Ghar El Melh surface sediment (May 2021). For sandy distribution (>0.063 mm) indexes are the Mode (Mo) and Median (Md) Mean in mm; in Phi scale: the Median (Mz); the phi standard deviation (σ, sorting) and the skewness (SKI) are calculated according to Folk and Ward (1957). D50 parameter is the mean value of the silty-muddy fraction (<0.063 mm). Depths are in meter.

	Samples	Depth	Mo	Md/D50	Mz	σ	SKI	Ku
Northern ridge	CB26	0 to -1	0.16	0,25	2,06	0,37	-0,04	0,75
	CB27	0	0.25	0,26	1,96	0,38	0,06	1,41
	CB28	+1	0.16	0,19	2,34	0,22	0,27	1,46
	CB29	0 to -1	0.16	0,24	2,09	0,38	-0,01	1,91
	CB30	0	0.16	0,24	2,09	0,38	-0,01	1,91
	CB31	+1	0.25	0,26	1,96	0,38	0,06	1,41
	CB32	0 to -1	0.25	0,24	2,08	0,28	-0,23	1,01
	CB33	0	0.16	0,24	2,09	0,28	-0,22	0,90
	CB34	+1	0.16	0,22	2,17	0,22	0,14	0,84
	CB35	0 to -1	0.25	0,28	1,80	0,11	0,82	4,74
	CB36	0	0.16	0,24	2,12	0,28	-0,26	0,74
	CB37	+1	0.16	0,18	2,41	0,55	0,51	3,08
Center	CB15	0 to -1	0.16	0,22	2,21	0,33	-0,15	1,00
	CB16	0	0.16	0,25	2,04	0,30	-0,23	1,00
	CB17	+1	0.16	0,19	2,30	0,30	0,30	0,99
	CB18	+1 to +3	0.16	0,23	2,12	0,35	0,03	0,71
	CB19	0 to -1	0.16	0,25	2,00	0,29	-0,13	1,09
	CB20	0	0.15	0,25	2,06	0,28	-0,33	0,63
	CB21	+1	0.15	0,23	2,11	0,36	0,12	0,81
	CB22	0 to -1	0.16	0,25	2,02	0,35	-0,11	0,81
	CB23	0	0.16	0,24	2,08	0,30	-0,07	0,81
	CB24	+1	0.16	0,24	2,04	0,27	0,04	0,74
	CB25	+1 to +3	0.16	0,20	2,36	0,30	-0,18	1,57
Southern ridge	CB1	0 to -1	-	0,0034	-	-	-	-
	CB2	0	0.16	0,22	2,18	0,35	0,00	0,78
	CB3	+1 to +3	0.16	0,25	2,06	0,37	-0,04	0,75
	CB4	0 to -1	016	0,19	2,35	0,33	0,12	1,04
	CB5	0	0.16	0,20	2,26	0,34	0,21	0,90
	CB6	+1	0.16	0,20	2,24	0,35	0,21	0,99
	CB7	0 to -1	0.16	0,20	2,32	0,35	0,00	1,03
	CB8	0	0.25	0,24	1,97	0,26	0,39	2,31
	CB9	+1	0.16	0,19	2,38	0,24	0,13	1,34
	CB10	+1 to +3	0.16	0,22	2,18	0,35	0,00	0,78
	CB11	0 to -1	0.16	0,21	2,18	0,37	0,17	0,83
	CB12	0	0.16	0,19	2,25	0,30	0,53	1,09
	CB13	+1	0.16	0,26	2,00	0,35	-0,17	0,86
	CB14	+1 to +3	0.16	0,25	2,05	0,40	-0,07	1,04

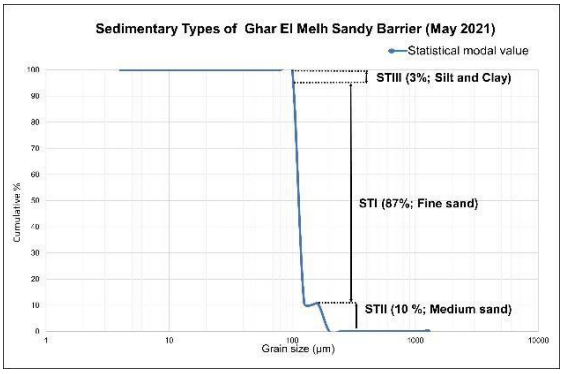

Figure 2. The Sedimentary Types Classification of the three Sedimentary Types (STI, STII, and STIII) of the subsurface sediment of the sandy barrier of Ghar El Melh (May 2021).

3.2. Quartz grain morphoscopy

The grain surface and shape observation of the 0.160 mm (STI) and 0.250 mm (STII) sieved sample shows that the sands (> 0.160 mm) are composed of four quartz roundness types, the (NU), (RM), (SA) and the (GB) (Figure 3 (A)). More than 50% of the sandy fraction is composed of blunted glow (BG) and subangular shape type. There are followed by the matt-rounded (RM) and fresh angular-NU types. A minor group of Ferruginous Surface Grains (FSG) is also present (Figure 3 (B)).

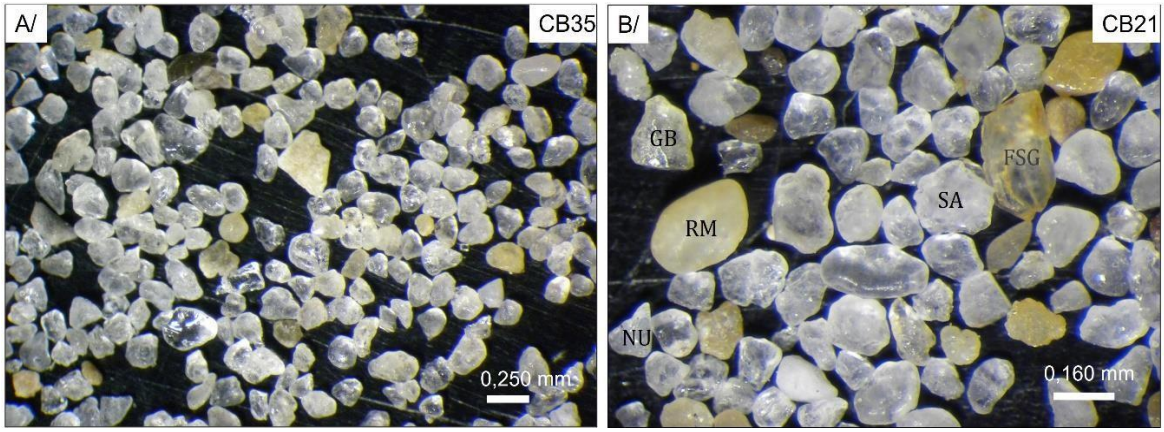

Figure 3. Morphoscopy of the quartz grain of the Ghar El Melh sandy barrier (May 2021). (A) CB35- Swash zone (0.25 mm); (B) CB21- Foreshore (Mo= 0160 mm).

3.3. Aeolian flux measurement and model comparison

The climatic conditions during the May 28, 2021, measurement campaign indicate that the wind's directions are coming from the northwest direction with an average speed of 17 km.h^{-1}. During May, the effective winds recorded are from the northwest to north-north-west direction with a frequency of 17 % (Figure 4). The winds that come from the northeast sector have a frequency of 6.5%, and the wind from the other directions has a negligible value. The measured flux rates Q_{mes} (kg.m^{-1}.mn^{-1}) of each run from the upper beach to the dune field and the semi-empirical model flux rate Q_{Cal} based on the shear velocity u* are shown in Table 3. Results suggest that the highest measured aeolian rate is at the summit of the dune in the center of the bay (profile 2) during the second hold of 15 min with a Q_{mes} value of 0.0022 kg.m^{-1}min^{-1}. We notice that the northward sandy ridge (profile 1) is almost null compared to the other two sites. The measured aeolian flux ranges of ~0.0005 kg.m^{-1}min^{-1} in the southern areas of the sandy barrier under a wind velocity ranged between 0.355 and 0.639 m.s^{-1} (Table 3). Grain particle analysis of the trapped sand reveals that Md equals ~0.006 mm.

The calculation of the Discrepancy Ratio for the Zingg formula (Dr=2.26) (Zingg, 1953) was adopted for the recorded Q_{mes}. The Bagnlod (1936) and Williams (1964) semi-empirical models annotated a Dr value of 12.94 and 41.90, respectively.

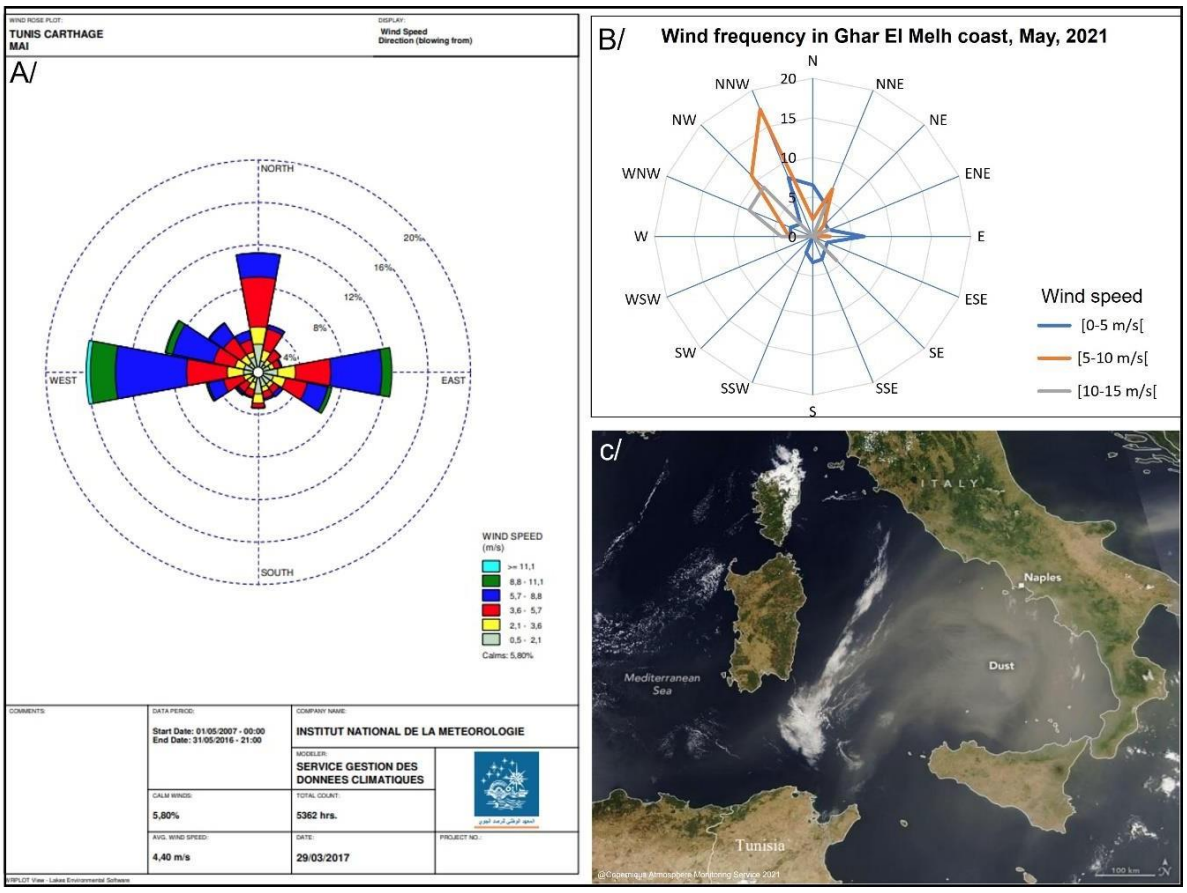

Figure 4. (A) Wind rose plot in the Gulf of Tunis. (B) Statistical wind frequency in Ghar El Melh coast during May 2021. (C) Dust storm satellite image captured by the Aqua satellite in May 2021 (Credit: @Copernicus Atmosphere Monitoring Service 2021, June).

Table 3. The measured flux rates Q_{mes} ($kg.m^{-1}.mn^{-1}$) of each run from the upper beach to the dune field and the semi-empirical model flux rate Q_{Cal} based on the shear velocity u*. Campaign 28 May 2021. UB: Upper beach; Dune feet: DF; Dune summit: DS; Blowout: B. Profile 1: Northern beach; Profile 2: Center of the bay; Profile 3: southern ridge of the sandy barrier. Wind friction speed u* ($m.s^{-1}$) was calculated from the reference altitude Zo (0.001 m, Arens, 1997) and the altitude above Z at the level of the beach of Ghar El Melh.

			Profile 1								Profile 2								Profile 3					
Time	Duration (mn)	Wind direction Speed (m.s-)	UB1		DF1		DS1		B1		UB2		DF2		DS2		B2		UB3		DF3		DS3	
			Q_{mes}	u*	Q_{mes}	u*	Q_{mes}	u*	Q_{mes}	u*	Q_{mes}	u*	Q_{mes}	u*	Q_{mes}	u*	Q_{mes}	u*	Q_{mes}	u*	Q_{mes}	u*	Q_{mes}	u*
10:00 to 10:20	20	NNW 9.7	0	0.639	0	0.594	0	0.496	0	0.56	0.0008	0.621	0.0008	0.607	0.0013	0.493	0.00107	0.543	0.0002	0.179	0.0003	0.584	0	0.487
10:30 to 10:45	15	NNW 9.7	0.0001	0.639	0	0.594	0	0.496	0	0.56	0.0012	0.621	0.0003	0.607	0.0022	0.493	0.00404	0.543	0.0001	0.179	0.0005	0.584	0	0.487
10:50 to 11:10	20	NNW 7	0	0.461	0	0.429	0	0.358	0	0.404	0.0001	0.448	0	0.438	0.0004	0.355	0.00001	0.392	0.0001	0.479	0.0001	0.421	0	0.351
11:15 to 11:45	30	NNW 7	0	0.461	0	0.429	0	0.358	0	0.404	0	0.448	0	0.438	0.0002	0.355	0	0.391	0.0001	0.479	0	0.421	0	0.351

4. Discussion

Coastal sandy barriers are among the most vulnerable low-lying landscapes to sea level rise (Vousdoukas et al., 2020). However, they are also significantly al., 2019). The lack of continental sand recharge and the modification of river impacted by anthropogenic inland drivers, such as the building of large dams, which trap mainly sand, preventing it from reaching the coast and participating in the beach accretion/renewing (Ben Moussa et regimes contribute to the alteration of the coastal geomorphology, as mentioned by

Amoussou's study (Amoussou, 2010) on the coast of Benin.

The sediment distribution of the barrier ridge of Ghar El Melh is typical to a wave-dominated coastal sandy barrier facies (Wright & Short, 1984). The grain size distribution of the subsurface sediment is composed of fine sand Sediment Type (STI) over the foreshore area (within an average tidal range of 0.4 m) and a medium sand type on the coastal dunes along the barrier. Toward the southern end of the embayment coast, the submerged bedforms are composed of a muddy distribution (<0.063 mm) i.e., STIII, found at depths of −1 m. According to Amrouni et al. 2020, the source of the mud originates from the historical deltaic deposit and the surrounding salt marshes submerged by the sea and reworked by the wave currents.

The sediment supply of the sandy coastal ridge is probably driven by the fluvial discharge carried out by the Medjerda River during the last centuries (Delile et al., 2015), with an amount of 60 to 80% of muddy component (El Arrim, 1996), and from the aeolian processes which a still unknown proportion. Sediments are also transported onshore by the longshore drift from the northeastern direction during the Winter season (Figure 1 (C)) and occasionally from the southeastern prevailing incident-wave direction in the summer season and stormy events (Amrouni et al., 2020). The observed blunted glow (BG) quartz grain in the intertidal zone (Figure 3 (A)) indicated the aquatic transport in both fluviatile and/or marine environments.

The shoreline evolution during the last century in the Ghar El Melh reveals a severe erosion rate exceeding -3.9 $m.yr^{-1}$ along the GMSB (Hzami, 2020; Hzami et al., 2021), which is manifested by a very high vulnerability to marine risks. This negative sedimentary imbalance will affect the progradation of the sandy barrier and reduce the length of the upper beach width and the height of the coastal foredunes. Moreover, the aeolian processes contribute to coastal sedimentation, especially in arid regions (Lokier et al., 2013). The round mat-RM and sub-angular quartz grain (SA) occurrence in the foreshore zone indicates the aeolian transport.

Even though the dissipative type of the Ghar El Melh beach, and the orientation of the coastline (~15%) to the incident wave, the maximum measured flux rate Q_{mes} is recorded in the center of the bay is about 0.0022 $Kg.m^{-1}min^{-1}$. The latter seems to be a marginal supply when compared to the Q_{mes} trapped in the Mahdia beach along the Gulf of Hammamet, on the middle eastern coast of Tunisia (Amrouni, 2008) within Q_{mes} equal to 0.1 $kg.m^{-1}min^{-1}$ in the coastal dune field. No aeolian flux is supplied by the northern sandy barrier upward the harbor dike management. The Median grain size is about 0.06 mm as the dam structures completely trap the sand particle (Amrouni & Mahé, 2021).

The aeolian flux quantification in the coastal sandy barrier of Ghar El Melh reveals insufficient sediment supplies. This study confirms the low sedimentation in the highly vulnerable coast, leading to a near coastal submersion of the sandy ridge “Coco Beach” (Figure 5).

5. Conclusions

The study of sedimentological and aeolian processes of the sandy barrier of Ghar El Melh in the gulf of Tunis suggests the dominance of the fine sandy distribution (Md =0.2 to 0.25 mm) in the foreshore areas from the swash zone to the coastal dune field. The muddy component is found on the nearshore areas at a depth of -1 m and corresponds to the old deltaic deposit of the Medjerda River.

Three Sedimentary types are identified: STI- fine sand in 87% of the cases, STII-

medium sand type (10%), and the muddy STIII found in the submerged deltaic bedforms within 3% of the total collected samples.

The aeolian quantification measurement reveals that very fine particles supplied only the center and the northern side of the barrier (Md= 0.006 mm). The maximum trapped flux rate Q_{mes} is ~ 0.0022 $kg.m^{1}min^{-1}$ on the dune summit. The Dr ratio establishes the validation of the Q_{mes}, and Zingg (1953) is the most adapted semi-empirical flux model (Q_{Cal}) of the sandy barrier of the lagoon.

Our results reveal the low or almost total lack of detrital supplies to the highly vulnerable coast of Ghar El Melh, leading to a near coastal submersion of the Ghar El Melh Sandy Barrier (GMSB). Immediate action is needed to protect the sandy beach before its total disappearance under the increased frequency of marine storms. In response to the above, the ECOVAL program (Amrouni et al., 2022) is exploring the efficiency of several Nature Based Solution, such as windbreakers, to mitigate the sediment imbalance and hopefully restore these unique coastal dunes.

Figure 5. The aerial view of the sandy barrier of Ghar El Melh, Gulf of Tunis, Tunisia, taken on 1st of December 2022, looking westward in the winter season.

Author Contributions

Conceptualization, Oula Amrouni; methodology, Abderraouf Hzami, Hodan Ibrahim Said and Essam Heggy; writing–original draft preparation: Oula Amrouni, data acquisition, and analysis: Hodan Ibrahim Said; writing–review and editing, Oula Amrouni and Essam Heggy; supervision, Oula Amrouni; project administration, Hechmi Missaoui; funding acquisition, Gil Mahé & Essam Heggy. All authors have read and agreed to the published version of the manuscript.

Funding

This study was conducted in the framework of the ECOCLIM -LR16 INSTM04 Institutional research program funded by the National Institute of Marine Sciences and Technologies, INSTM, University of Carthage, and the Tunisian Ministry of Higher Education and Scientific Research in Tunisia.

Acknowledgments

The authors are grateful for the helpful discussions with several members of the Laboratory of Mineral Resources and Environment, Faculty of Sciences, the University of Tunis El Manar, Tunisia.

Conflicts of Interest

The authors declare no conflict of interest.

References

1. Amoussou E. (2010). *Variabilité pluviométrique et dynamique hydro-sédimentaire du bassin-versant du complexe fluvio-lagunaire Mono-Ahémé-Couffo (Afrique de l'Ouest)*. [Thèse de Doctorat, Université de Bourgogne, France], 305 p. https://theses.hal.science/tel-00493898v2
2. Amrouni O., Mahé G., Hzami A., Marouani, M.A. & Missaoui H. (27-30 November 2022). Ecosystemic services tool for a better Conservation and Valorization of coastal Lagoon: ECOVAL. *Mediterranean Geosciences Union Annual Meeting (MedGU-22)*, Marrakech, Morocco.
3. Amrouni O. (2008). *Morphodynamique d'une plage sableuse microtidale à barres: côte nord de Mahdia (Tunisie orientale)*. [Doctorat de Géologie, Université de Tunis El Manar], http://hdl.handle.net/1834/5443
4. Amrouni O., Beji Y., Heggy E. & Sánchez A. (2-5 Nov. 2020). Coastal Sedimentary dynamic of wetland ecosystem of semi-arid areas in north Africa. *3rd Conference of the Arabian Journal of Geosciences*.
5. Amrouni O. & Mahé G. (24-28 Nov. 2021). Multi-criteria approaches to identify the shoreline retreat downstream of dams: the North African case. *Proceeding 4th International Conference on the "Hydrology of the Great Rivers of Africa"*. Cotonou, Bénin.
6. Amrouni O., Sánchez A., Khélifi N., Ben Moussa T., Chiarella D., Mahé G., Abdeljaouad, S. & McLaren, P. (2019a). Sensitivity assessment of the deltaic coast of Medjerda based on fine grained sediment dynamics, Gulf of Tunis, Western Mediterranean. *Journal of Coastal Conservation*, 23, 571-587. https://doi.org/10.1007/s11852-019-00687-x
7. Arens S.M. (1997). Patterns of sand transport on vegetated foredunes. *Geomorphology*, 17(4), 339-350. https://doi.org/10.1016/0169-555X(96)00016-5
8. Bagnold R. A. (1941). *The physics of blown sand and desert sand*. Methuen, London. 266 p.
9. Barusseau J. P. (2011). Influence of mixtures of grain-size populations on the parametric and mode characteristics of the coastal sands (Hérault, Mediterranean Sea, France). *Journal of Sedimentary Research*, 81(8), 611-629. https://doi.org/10.2110/jsr.2011.46
10. Ben Moussa T., Amrouni O., Hzami A., Dezileau, L., Mahe G., Condomines, M. & Saadi A. (2019). Progradation and retrogradation of the Medjerda delta during the 20th century (Tunisia, Western Mediterranean). *Comptes Rendus Geosciences*, 351(4), 340-350. https://doi.org/10.1016/j.crte.2018.10.004
11. Cailleux A. (1942). Les actions éoliennes périglaciaires en Europe, *Mémoires de la Société géologique de France*. 46, 1-176.
12. Corbau C., Greco M., Martino G., Olivo E. & Simeoni U. (2022). Assessment of the Vulnerability of the Lucana Coastal Zones (South Italy) to Natural Hazards. *Journal of Marine Science and Engineering*, 10 (7), 888. https://doi.org/10.3390/jmse10070888
13. Delile H., Abichou A., Gadhoum A., Goiran J.P., Pleuger E, Monchambert, J-Y, Wilson A., (2015). The Geoarchaeology of Utica, Tunisia: The Paleogeography of the Mejerda Delta and Hypotheses Concerning the Location of the Ancient Harbor. *Geoarchaeology*, 30 (4), 291-306. https://doi.org/10.1002/gea.21514
14. Edward J. Anthony. (2008). Chapter Five Sandy Beaches and Barriers. In: *Developments in Marine Geology*, Elsevier, 4, 159-288. https://doi.org/10.1016/S1572-5480(08)00405-3
15. El Arrim A. (1996). Étude d'impact de la dynamique sédimentaire sur la stabilité du littoral du Golfe de Tunis. [Thèse de Doctorat de Géologie, Université de Tunis El Manar].
16. Folk R. L. & Ward W.C. (1957). Brazos River bar, a study in the significance of grain size parameters. *Journal of Sedimentary Petroology*, 27(1), 3-26,

https://doi.org/10.1306/74D70646-2B21-11D7-8648000102C1865D
17. Hzami A. (2021). *Etude morphodynamique du système littoral face aux changements climatiques et à l'élévation du niveau de la mer (Golfe de Tunis, mer Méditerranée),* [Thèse de doctorat, Université Tunis el Manar, Tunis]. http://hdl.handle.net/1834/41984
18. Hzami A., Heggy E., Amrouni O., Mahé, G., Maanan M. & Abdeljaouad S. (2021). Alarming coastal vulnerability of the deltaic and sandy beaches of North Africa. *Scientific Reports*, 11, 2320. https://doi.org/10.1038/s41598-020-77926-x
19. INM - Tunisian Meterorological Institute. (2019). Climatological data from Tunis station. https://www.meteo.tn/fr/institut-national-de-la-meteorologie
20. INM - Tunisian Meterorological Institute. (2020). Climatological data from Tunis station. https://www.meteo.tn/fr/institut-national-de-la-meteorologie
21. IPCC (2022). *Climate Change 2022: Impacts, Adaptation and Vulnerability*. Contribution of Working Group II to the Sixth Assessment Report of the Intergovernmental Panel on Climate Change [H.-O. Pörtner, D.C. Roberts, M. Tignor, E.S. Poloczanska, K. Mintenbeck, A. Alegría, M. Craig…(eds.)]. Cambridge University Press. https://doi:10.1017/9781009325844
22. Komi, A., Petropoulos A., Evelpidou, N., Poulos S. & Kapsimalis V. (2022). Coastal Vulnerability Assessment for Future Sea Level Rise and a Comparative Study of Two Pocket Beaches in Seasonal Scale, Ios Island, Cyclades, Greece. *Journal of Marine Science and Engineering*, 10(11), 1673. https://doi.org/10.3390/jmse10111673
23. Krasnov H., Katra I. & Friger M. (2016). Increase in dust storm related PM10 concentrations: a time series analysis of 2001-2015. *Environmental Pollution*, 213, 36-42. https://doi.org/10.1016/j.envpol.2015.10.021
24. Krumbein W.C. (1941). Measurement and geological significance of shape and roundness of sedimentary particles. *Journal of Sedimentary Petrology*, 11, 64-72.
25. Lazzari N, Becerro M.A., Sanabria-Fernandez J.A. & Martin-Lopez B. (2021). Assessing social-ecological vulnerability of coastal systems to fishing and tourism. *Science of the Total Environment*, 784. 147078. https://doi.org/10.1016/j.scitotenv.2021.147078
26. Leatherman S. P. (1978). A new aeolian sand trap design. *Sedimentology*, 25(2), 303-306. https://doi.org/10.1111/j.1365-3091.1978.tb00315.x
27. Lokier S.W., Knaf A., Kimiagar S. (2013). A quantitative analysis of Recent arid coastal sedimentary facies from the Arabian Gulf Coastline of Abu Dhabi, United Arab Emirates, *Marine Geology*, 346, 141-152. https://doi.org/10.1016/j.margeo.2013.09.006
28. Paskoff R. (1994). Le delta de la Medjerda (Tunisie) depuis l'Antiquité. *Études Rurales,* n°133-134- Littoraux en perspectives, 15-29. https://doi.org/10.3406/rural.1994.3451
29. Pimenta J. (1959). Le cycle Pliocène actuel dans les bassins paraliques de Tunis. *Mémoires de la Societé Géologique de France*, Nouvelle Série, Tome XXXVIII (Fasc. 1), Mémoire n° 85.
30. Shepherd M. & Hesp P. A. (2003). Sandy barriers and coastal dunes. In: Giff, J.R. (Ed.), *The New Zealand Coast: Te Tai O Aotearoa*. Dunmore Press, Palmerston North, 163-190.
31. Sherman D.J. & Bauer, B.O. (1993). Dynamics of beach-dune systems. *Progress in physical geography: Earth and Environment,* 17(4), 413-447. https://doi.org/10.1177/030913339301700402
32. Kármán Th.V. (1921). Uber laminare und turbulente reibung. *ZAMM- Journal of Applied Mathematics and Mechanics/ Zeitschrift für Angewandte Mathematik und Mechanik*, 1(4), 233-252. https://doi.org/10.1002/zamm.19210010401

33. Vousdoukas M. I., Ranasinghe R., Mentaschi L., Plomaritis Th., Athanasiou P., Luijendijk A. & Feyen L. (2020). Sandy coastlines under threat of erosion. *Nature Climate Change*, 10, 260-263. https://doi.org/10.1038/s41558-020-0697-0
34. Williams G. M.A. (1964). Some aspects of aeolian transport load. *Sedimentology*, 3, 257- 287.
35. Wright L. D., Short. A.D. (1984). Morphodynamic variability of surf zones and beaches: a synthesis. *Marine Geology*, 56 (1-4), 93-118. https://doi.org/10.1016/0025-3227(84)90008-2
36. Zingg A. W. (1953). Wind tunnel studies of the movement of sedimentary material. In: *Proceedings, 5th Hydraulics Conference, Studies in Engineering*, 34, 111-135.